Chapter

Progress on Experimental Study of Melt Pool Flow Dynamics in Laser Material Processing

Xianfeng Xiao, Cong Lu, Yanshu Fu, Xiaojun Ye and Lijun Song

Abstract

Laser material processing has becoming a rapid developing technology due to the flexibility of laser tool. Melt pool is the main product from the interaction between laser and material and its features has a great impact on the heat transfer, solidification behavior, and defects formation. Thus, understanding changes to melt pool flow is essential to obtain good fabricated product. This chapter presents a review of the experimental studies on melt pool flow dynamics for laser welding and laser additive manufacturing. The mechanisms of melt pool convection and its principal affecting factors are first presented. Researches on melt flow visualization using direct and indirect experimental methods are then reviewed and discussed.

Keywords: Laser welding, Laser additive manufacturing, Melt pool, Convection flow

1. Introduction

Replace the entirety of this text with the introduction to your chapter. The introduction section should provide a context for your manuscript and should be numbered as first heading. When preparing the introduction, please bear in mind that some readers will not be experts in your field of research.

Since laser was invented by Maiman in 1960, it has experienced rapid applications in laser material processing. The advantages of high quality, high precision, high efficiency and high flexibility promote laser welding and laser additive manufacturing becoming the best developing foreground technologies in welding areas and additive manufacturing domains, respectively. Unlike arc welding, laser welding creates small melt pool with a high intensity laser beam spot, which allows the achievement of smooth welding seam with narrow heat affected zone (HAZ) and low distortion. The noncontact feature of laser also frees the welder from harshest environments. Laser additive manufacturing's equipment and parameters share many common features with laser welding. Laser additive manufacturing can be considered by extending laser welding from two-dimension seam to three-dimension bulk with a synchronous powder or wire feeding. According to the ASTM F42 Committee [1], the laser powder bed fusion (LPBF) and laser directed energy deposition (L-DED) are the two most relevant laser additive manufacturing process.

The essence of laser material processing is laser interact with materials, either heat or melt, or ablation. Irradiated by a laser beam, the localized material undergoes a rapid heating–cooling thermal cycle. Melt pool is the main product from the interaction between laser and materials, both for laser welding and laser additive manufacturing. Melt pool temperature field and its evolution determine the temperature gradient (G) and solidification rate (R). Together, G and R determine the solidification morphology and the microstructure scale [2]. Namely, GR determines the scale of microstructure, their ratio G/R is linked to the morphology of solidified microstructure, thereby affecting the mechanical properties of the weld seam or fabricated part. In addition, melt pool geometry including its size and shape also affects solidification behavior. A wide and shallow melt pool beneficial to the epitaxial growth of grains along one direction, resulting in a strong texture. Melt pool dimension is also found correlated to residual stress in selective laser melting [3]. Such melt pool characteristics has been reviewed by Yan et al. [4], by Fotovvati et al. [5] and Willy et al. [6].

Another often overlooked melt pool characteristic is flow dynamics. Due to the small timescales and highly transient of the melt flow, it is very difficult to reveal dynamic behavior inside the melt pool. The flow in melt pool is mainly derived by spatial variation of the surface tension, which is known as thermocapillary flow or Marangoni convection, named after Italian Physicist Carlo Marangoni. Prior studies have shown that fluid flow plays an important role in heat transfer and solidification behavior in the melt pool, thus significantly affect the melt pool geometry, solidification microstructure, alloy element distribution, surface roughness and defects formation. Therefore, comprehensive understanding of the evolution of melt flow is a key concern and hot topic to improve the product quality during laser welding and laser additive manufacturing processes.

Melting of metals is commonly found various industrial applications, such as arc welding, metal casting and laser processing. Analysis of melting can be described as the Stefan problem assuming a heat conduction-controlled process; that is, fluid flow in molten pool is neglected. The effects of weld fluid flow induced by surface tension was first proposed in late 1960s [7]. From then on, various experimental and numerical investigations concerning fluid flow in laser melt pool have been reported in the open literature. Because of the small size of the weld pool and high dynamics, real-time experimental measurement of temperature and velocity fields inside the melt pool is very challenging. Therefore, mathematical modeling is the main research method to predict and describe the melt pool behavior. Mazumder [8] and Cook [9] have reviewed the approaches to incorporate melt convection effects as well as melt pool behavior during laser welding and laser additive manufacturing. However, quantitative investigations of flow pattern and velocity inside melt pool by experiment are still needed to validate the models. Recent developments in high-speed photography, image processing technology and the third-generation synchrotron radiation sources have enabled researchers to characterize the time-transient fluid flow inside the melt pool. Those research efforts are critical to reveal flow evolution and offers the possibility to calibrate or verify advanced numerical models.

This chapter aims to provide a comprehensive review of the experimental progress on melt pool flow dynamics for laser material processing, focusing on laser welding and laser additive manufacturing. The formation mechanism and driving forces for laser melt fluid flow is firstly introduced. Principal affecting factors for melt fluid flow are analyzed from open literature. The experimental results of laser melt fluid flow are reviewed and discussed, aiming at providing a fundamental understanding of melt flow convection mechanisms.

2. Forces within the melt pool and its effect factors

2.1 Driving forces in melt pool

The melt pool flow dynamics depends on the forces acting on the melt volume, thus the force analysis is crucial to investigate the formation mechanism of weld geometry, solidification microstructure, surface roughness and defects. The schematic diagram of forces on melt pool is shown in **Figure 1**. In the liquid melt pool during laser welding and laser additive manufacturing, there are four principal forces acting on the fluid flow: buoyancy force (originate from the spatial variation of the liquid-metal density), Marangoni force (originate from surface tension gradients), gravity and shear force (originate from laser induced vapor or plasma). In the case of applying an auxiliary electric or magnetic field, electromagnetic force on liquid melt pool should be also considered. Moreover, when evaporation occurs in the keyhole melting mode, recoil pressure becomes the principal driving force of molten metal. These driving forces and the interplay between them induce the complex flow motion in the melt pool.

Buoyancy force originate from the spatial variation of the liquid-metal density, mainly because of temperature variations, and, to a lesser extent, from local composition variations. It is known that density is a function of material's temperature, namely density decreases with increasing temperature. The temperature of liquid metal in the upper of the melt pool is higher than the bottom of the melt pool, leading to an upward movement of the melt pool as shown in **Figure 2**. Experimental [10] and numerical model [11] results have shown that buoyancy effect can be negligible when compared to Marangoni force in laser melting. The convection flow

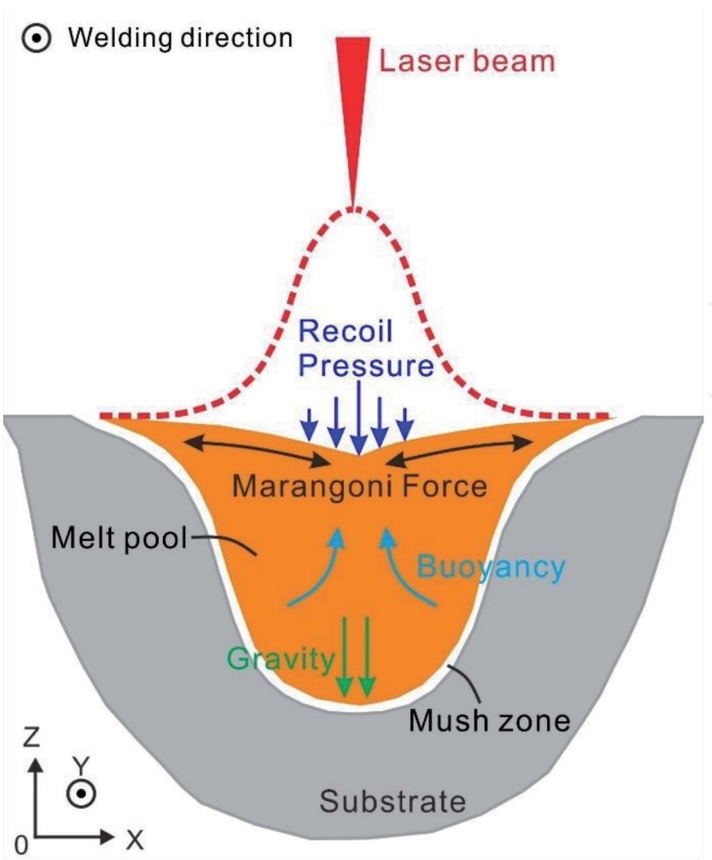

Figure 1.
Fluid forces acting on the weld pool.

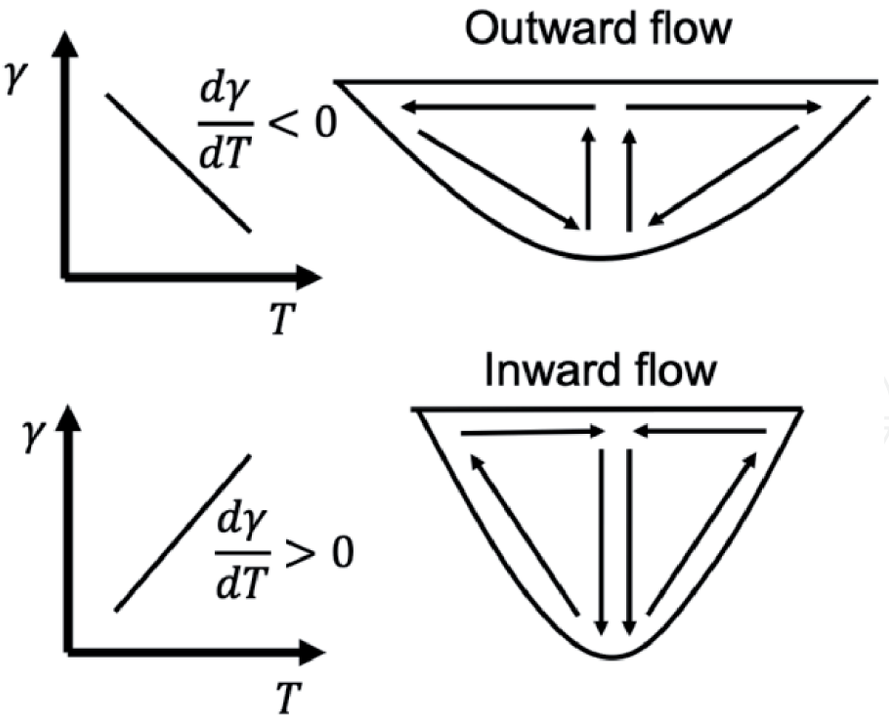

Figure 2.
Effect of the sign of the surface tension temperature coefficient on fluid flow in the weld pool.

caused by gravity is in the direction against the buoyancy force. Simulation results showed that gravity has no noticeable influence on the dimensions and shapes weld pool when laser welding a flat plate. However, when welding applied in circumferential condition or horizontal condition or near vacuum condition. The influence of gravity on the melt flow plays a critical role. The orientations of weld pools relative to gravity are different for different welding positions. For flat welding, gravity only contributes to the fluid flow in plate thickness direction. For inclined or horizontal welding, the melt pool is shifted afterwards under gravity action. Poor weld formation quality (unstable, porosity and undercut) is more likely to be developed [12]. Guo et al. demonstrated that full penetration of thick plate in horizontal position can mitigate some of the common welding defects including undercut and sagging [13].

One of the important aspects of laser welding and laser additive manufacturing is the convection driven by Marangoni force, also known as thermocapillary. The Marangoni force acts as a shear stress at the free surface thereby inducing convective flow within the molten pool. The driving mechanisms of surface tension can generally be classified as: temperature gradient, concentration gradient, pH gradient, surfactant-induced flow, and so on. Among these origins, temperature gradient is considered as the main driving forces of fluid flow in laser melting pure metals and most alloys. When laser locally heats the plate surface, the highest temperature located in the center of melt pool and decreases radially, causing a surface tension difference in the melt pool and thus creating an outward melt flow. A considerable amount of studies have showed the dominance of Marangoni force in the conduction mode melt pool convection.

Generally, two laser melting mechanisms: the conduction and the keyhole (deep penetration) mode are used. Recently, they are also adapted in laser additive manufacturing. Qualitative distinction of conduction mode and keyhole mode is whether evaporation happens or not. Once evaporation takes place, the vapor pressure (recoil pressure) acts like a piston on the liquid melt pool. The recoil pressure tends to push the liquid towards the pool edge and keyhole forms. Recoil pressure is widely accepted to be the principal driving force for fluid flow in the keyhole melting.

Besides the above-mentioned driving forces in melt pool, external force could be also introduced. For example, shielding gas in laser welding could help reduce surface oxidation and stabilize the melt pool fluctuations. It will also exert pressure on melt pool and alter the flow pattern in the molten pool. Electromagnetic force may be introduced via applying an electromagnetic compound field to the molten pool.

2.2 Factors affecting melt pool convection

According to the above force analysis in melt pool, surface tension and recoil pressure are the dominate driving mechanisms for melt pool convection. Processing parameters of laser welding and laser additive manufacturing can be classified into four types: laser related parameters, scan related parameters, gas/powder-related parameters, material-related parameters.

2.2.1 Laser related parameters

Laser energy density is considered as one of the most significant variables on temperature field and material evaporation. Laser power, beam spot size, pulse frequency and energy distribution jointly determine the laser energy density. In conduction mode, the higher laser power leads to the larger temperature gradient in melt pool, resulting in higher surface tension and more intense radially convection. With the laser power increased, the input laser energy increased which caused an intense evaporation and the keyhole forms. Therefore, recoil pressure takes over as the primary driving force, pushing melt flow along the thickness direction.

2.2.2 Scan related parameters

For stationary laser welding, laser induced temperature field is axisymmetric resulting in an axisymmetric weld pool and keyhole. When laser moves with a certain velocity, temperature gradient in the front side of the moving laser beam is much steeper than that in the rear side. The melt pool shape resembles as in comet tail profile. Reducing laser scanning speed will cause the interaction time and peak temperature to increase substantially. As a result, increased temperature gradients lead to stronger Marangoni fluid convection and larger area of the molten pool. Laser oscillating welding is founded stabilize the fluid flow in melt pool and keyhole [14]. As for laser additive manufacturing of 3D bulks, scanning pattern, hatch spacing and layer thickness influence melt pool behavior through fore layers.

2.2.3 Gas/powder-related parameters

In laser welding, side shielding gas serves three purposes: prevent the weld from oxidizing, remove the plasma plume and stabilize melt pool and keyhole. However, the too large flow rate of shielding gas gives resultant strong pressure on the melt pool and increases the fluctuation of the weld pool, keyhole and plasma. Thus, an optimal gas flow rate of shielding gas for a stable welding process is needed. For laser additive manufacturing, the main function of shielding gas is preventing melt pool from oxidizing. In DED process, typical average particle velocity is on the order of 5–10 m/s. The blown powder particles with low temperature impinging on the melt pool will change melt pool temperature field. In addition, impact force of powder particles may affect both the flow pattern and penetration of melt pool.

2.2.4 Material-related parameters

As mentioned previously, the melt flow in the pool is driven by surface tension gradients due to temperature gradients. The direction of the Marangoni flow is dictated by the sign of the surface tension gradient and is shown in **Figure 2**. For pure metals the surface tension coefficient is constant negative, therefore creating an outward radial flow (see **Figure 2(a)**). In 1982, Heiple and Ropper [15] found that the presence of surfactants in arc welding molten materials can alter Marangoni convection in the melt pool, and thus creating an inward radial flow (see **Figure 2(b)**). They also proposed that the Marangoni convection is the most important factor in determining weld shape, but without quantitative description of surface tension phenomenon. Sahoo et al. [16] were the first to propose a semi-empirical relationship between the surface tension gradient, temperature and content of surface-active elements, for various binary alloys. For a Fe-S binary alloy, at a certain of sulfur content, a critical temperature exists which corresponds to a change in the sign of the surface tension gradient, and results in a flow reversal, creating simultaneously two different vortices. Surfactant elements such as S, Se, Te, O can be added in the form of substrate, gas, wire or powder.

3. Experimental studies for melt pool flow investigation

Since surface tension driven weld fluid flow was first reported in 1965 [7], a number of experiment have been conducted to investigate the melt pool flow in laser welding and laser additive manufacturing. Melt pool flow investigation can be classified into indirect and direct approaches. Indirect methods by means of postmortem analysis of the cross sections of fusion zones are often used to infer the melt flow patterns. According to the employed equipment, direct observation of melt flow can be divided into three stages (see **Figure 3**): (1) 1970s ~ 2000s, use simulated material to visualize melt flow pattern; (2) 2000s ~ 2015s, employ high-speed camera and X-ray tube transmission system; (2) 2015s ~ to date, apply the third-generation synchrotron radiation sources for in-situ high-speed high-energy x-ray imaging.

3.1 Indirect analysis of the fluid flow

Melt flow convection in the weld pool will drive material transport in the weld. Indirect methods by means of postmortem analysis of the cross sections need tracers to identify the melt flow patterns. One way to analysis the melt flow pattern is using tracing particles with high hardness such as W, ZrO_2, SiC, TiB_2. Schemed as **Figure 4**, tungsten particles are pre-paved on the substate and two tungsten

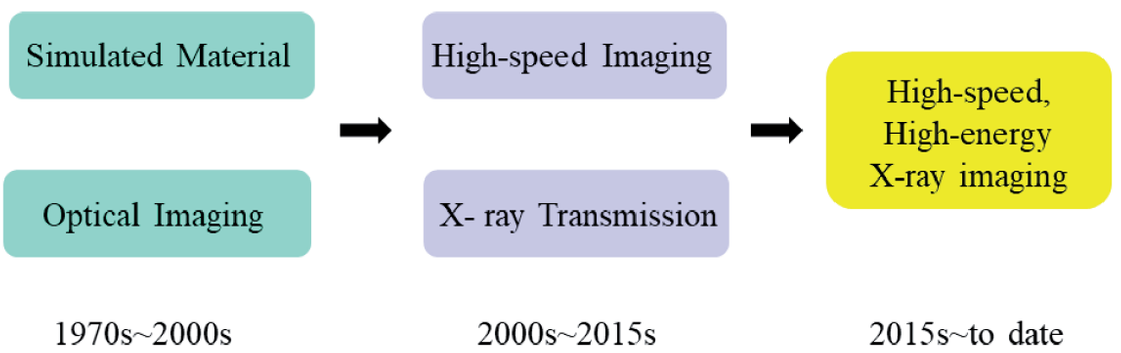

Figure 3.
Development of the experimental studies for direct observation of melt pool flow.

plates are inserted into the substate. After welding, microhardness distribution in the cross sections is measured. In the case of outward melt flow (**Figure 4(a)**), microhardness outside the plates is higher than that of between the plates. While for inward melt flow (**Figure 4(a)**), microhardness between the plates is higher than that of outside the plates. Li et al. [17] used this method to investigate the effect of shielding gas on TIG welding melt flow. Due to the high aspect ratio of welds in laser welding, it is difficult to insert two tungsten plates inside the substrate.

In 2005, Thomy and Vollertsen from BIAS [18] introduced a sandwich structure with a thin copper sheet between two aluminum sheets to study effects of magnetic fields on laser melt flow, see **Figure 5(a)**. With the help optical microscopy, hardness tester and EDX, darker region in **Figure 5(b)** and **(c)** is confirmed with higher copper content. Thus, the authors draw a conclusion that magnetic stirring induced by alternating magnetic fields promotes welds homogeneity. Beside using particles or metal sheet (Cu or Ni) as tracers, other forms of tracers such as filler has also been used [19].

3.2 Simulated materials for direct flow visualization

At the beginning, paraffin wax was employed to understand Marangoni flow in gas tungsten arc welding (GTAW). Ishizaki et al. [7] used a soldering iron to locally heat the surface of a thin slice of molten paraffin, circulation in the pool was observed by monitoring the movement of graphite particles. The resulting solidified structure that had a cross-sectional morphology similar to that of static GTAW welds. Similar Marangoni flow phenomena has also been found by using mercury [20], stearic acid [21], ice or water [22].

Simulated materials used above were applied in arc welding and only surface flow was visualized. For laser welding, it has a smaller size of melt pool and electromagnetic force does not exist. The physically simulated laser weld pool was first investigated by Limmaneevichitr and Kou from University of Wisconsin [23, 24]. Sodium nitrate, NaNO3, was chosen as it is transparent and exhibited similar surface properties to those seen in metal welding. In their experiment, a defocused CO_2 heat

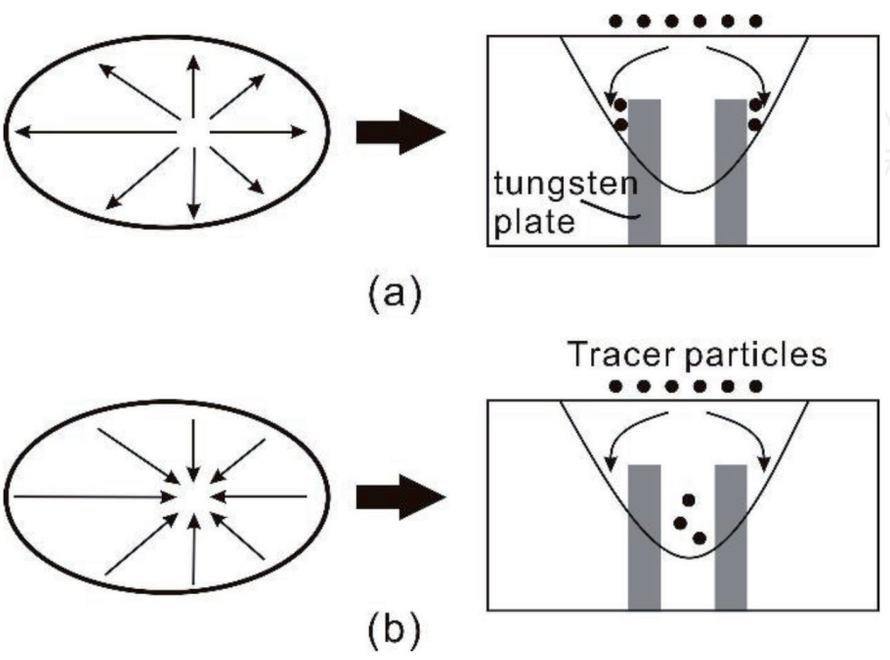

Figure 4.
Tracing particle distribution under (a) outward and (b) inward of Marangoni convection.

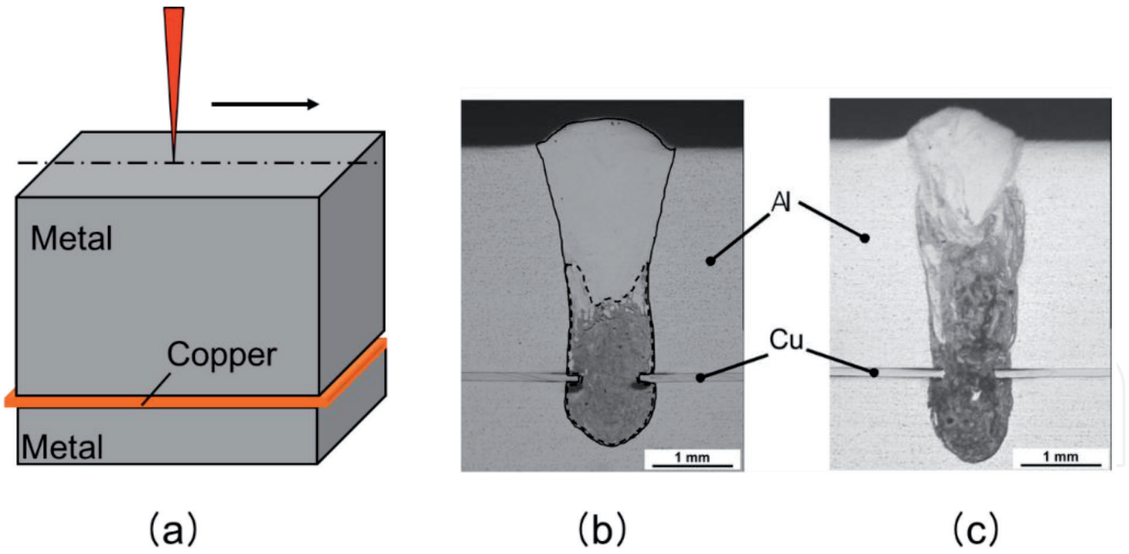

Figure 5.
(a) Scheme of sandwich structure with a thin copper sheet between two aluminum sheets; weld cross section with (b) omT and (c) 60 mT of alternating magnetic field [18].

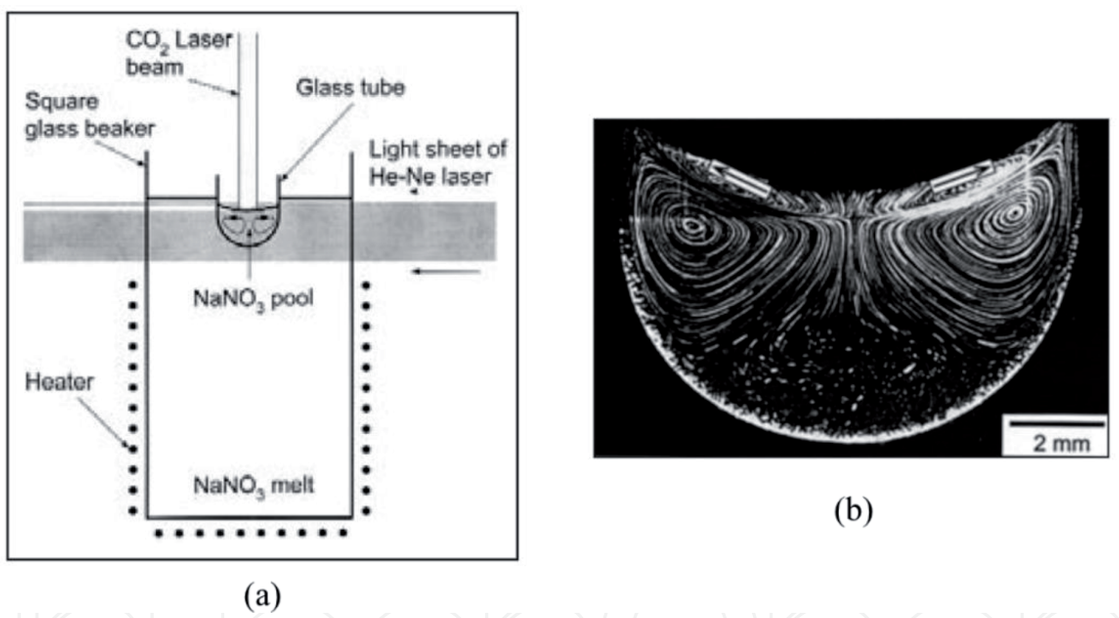

Figure 6.
(a) Experimental set up and (b) Visualization of Marangoni flows in a laser generated pool in a vat of $NaNO_3$ [23].

up the NaNO3 and another He-Ne laser light sheet, either vertical or horizontal, to cut through the pool to illuminate the tracer particles suspended in the pool and reveal the flow pattern, show in **Figure 6**. Also, to visualize the reversal flow pattern inside the weld pool, they used a transparent pool of NaNO3 with C_2H_5COOK as the surface-active agent [24]. This finding proved what was proposed by Heiple and Roper [15] in arc welding: a minor presence of surface-active elements can substantially change the temperature dependence of surface tension, leading to a change in flow pattern.

Another important driving force for melt flow is recoil pressure in the case of keyhole mode welding. Keyhole phenomenon is more complex and transient, due to fierce evaporation. The keyhole mode welding can be thermodynamically unstable and causes the formation of defects such as porosity, spatter, hump and undercut. Although direct observation of the keyhole is not easy, many efforts have been made. A low cost method for direct observation of keyhole and its evolution is

welding transparent glass. Overall, there are three typical configurations with glass for keyhole observation: (1) directly welding on glass; (2) using sandwich structure consisting a metal foil between two glass plates; (3) using metal/glass structure. Schematic of the three configurations is shown in **Figure 7**.

The first image of keyhole was captured by Arata et al. in 1976, by welding in a soda-lime glass (**Figure 8(a)**). A similar approach was used on GG17 glass, which with an excellent heat-resistance property [25]. Sandwich structure consist of a metal foil between two glass plates (see **Figure 8(b)**) was first reported by Kato et al. [26] in 1985 in laser drilling. Zhang et al. used the sandwich structure approach to measure plasma inside keyhole [27]. It's worth noting that welding in glass (**Figure 8(a)**) and sandwich structure (**Figure 8(b)**) is far different from actual laser welding of compact metal. For welding in glass, physical and thermal properties of glass differ greatly from metallic engineering materials. For welding in sandwich structure, the loose multilayer construction is liable to cause keyhole collapse, which affects the stability of the welding process and could lead to misleading results. In 1994, Semak et al. [28] introduced a laser welding metal-glass approach to obtain transient keyhole profile, see **Figure 8(c)**. The penetration depth in real laser welding metal is used to calibrate the position of the laser beam center relative to the metal-glass interface. Suffering from limited high-speed imaging resolution, only low contrast keyhole profile was obtained. Nowadays, the rapid development of the high-speed imaging technology made it possible to observe the highly transient keyhole clearly. Zhang et al. [29] used a metal-glass samples which consists of one sheet of stainless steel and one piece of GG17 glass to directly observe the deep penetration welding keyhole, see **Figure 8(c)**. With the help of a high speed camera, a clear image of the keyhole wall was captured, shown as **Figure 8**. In recent years, the metal/glass structure approach is widely used to study keyhole dynamics and welding defects formation mechanisms [30, 31].

3.3 High speed imaging of tracers

It is worth noting that both the element tracing method and simulated material method can only drive quantitative conclusions. Addition, element tracing method can only obtain the final state of melt flow, lacking of transient information. Laser

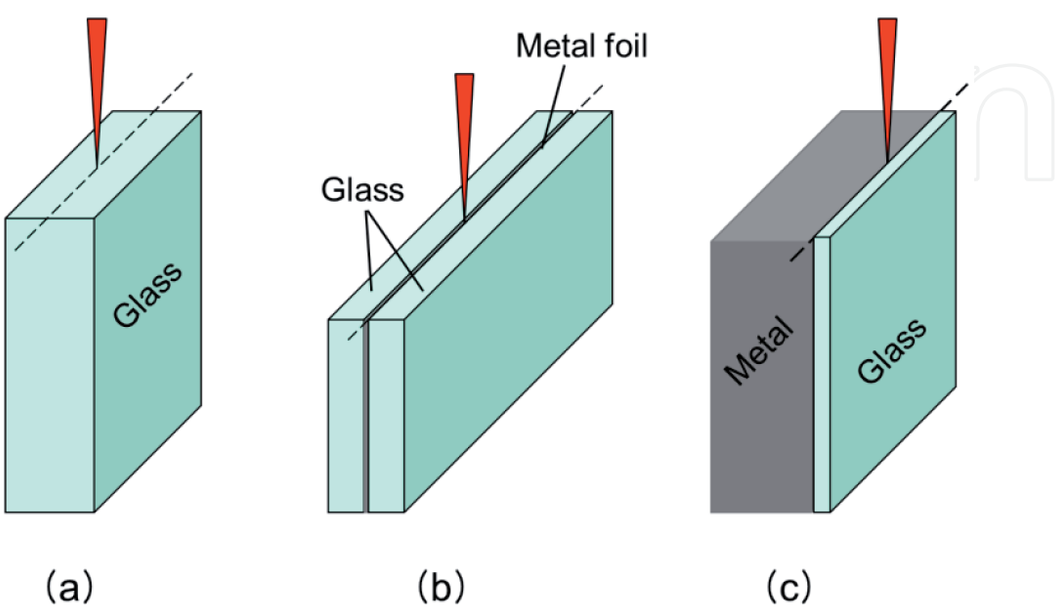

Figure 7.
Three typical configurations of keyhole observation for laser welding in: (a) glass, (b) glass/foil/glass, (c) metal/glass.

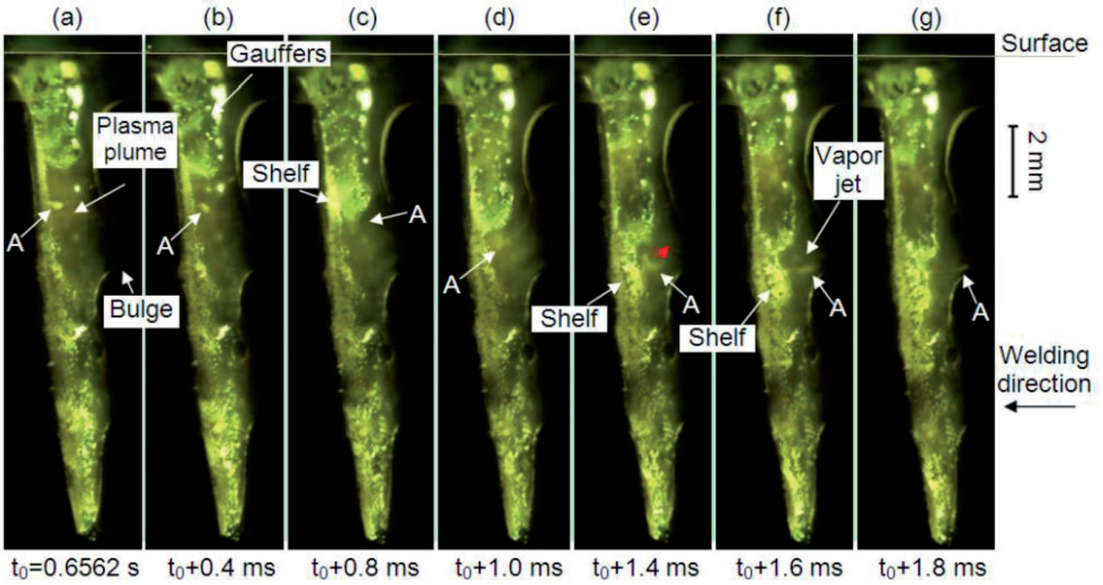

Figure 8.
Clearly keyhole images captured by laser welding metal/glass structure, (a)-(g) with a interframe time of 0.4 ms [29].

weld pool flow dynamics have been studied by simulation for many years since it is difficult to visualize transient flows in such a tiny zone. With the rapid development of high speed camera equipment and imaging processing technology, researchers can now capture highly transient melt flow.

Since melt flow velocity in laser melting can be of the order of 1 m/s [32, 33], successive images of a single tracer should be captured in a time interval shorter than 1 ms, corresponds to a minimum frame rate of 1000 fps. Therefore, imaging frame rate must be kept in the multi-fps range. In order to capture higher resolution and large viewing areas of melt pool, external illumination with narrow band interference filter is necessary. This technique reduces greatly the effect of laser induced vapor or plasma radiation.

To quantify the melt flow velocity, tracer-based flow measurement methods are wildly used. The tracer could either be "nature", that is to say belong to the weld pool (such as surface oxide particles, humps, slag particles), or 'artificial' particles, added by the experimenter. Calculation of melt flow velocity is by measuring the distance between the tracer in two successive images divided by the interval time. For low density of tracers, particle tracking velocimetry (PTV) algorithm is applicable. While for moderate density of tracers, particle image velocimetry (PIV) is widely been used by tracking groups of tracers and performing a cross-correlation calculation on successive images. In the case of a very high density of tracers, optical flow type of approach is needed. Ki et al. [32] use a hump as the tracer to measure the melt flow velocity, shown as **Figure 9**. The authors assumed that the velocity of hump is close to the actual flow velocity. Thus, the experimentally obtained weld melt flow velocity were in the range of 1.4 to 2.2 m/s.

However, PTV-based method can only obtain several path lines in a flow field. In order to get the whole picture of melt flows, more "nature" or 'artificial' tracers are needed. Wirth et al. [33] used particles tacking method to obtain melt pool surface flow field. The results shown that using metal powder particles as tracers has a qualitatively similar flow field with using carbide or oxide particles as tracers, shown as **Figure 10**. The flow lines arisen from the center of melt poot point to its edge indicates that melt flow is driven by Marangoni force caused by temperature gradient in L-DED.

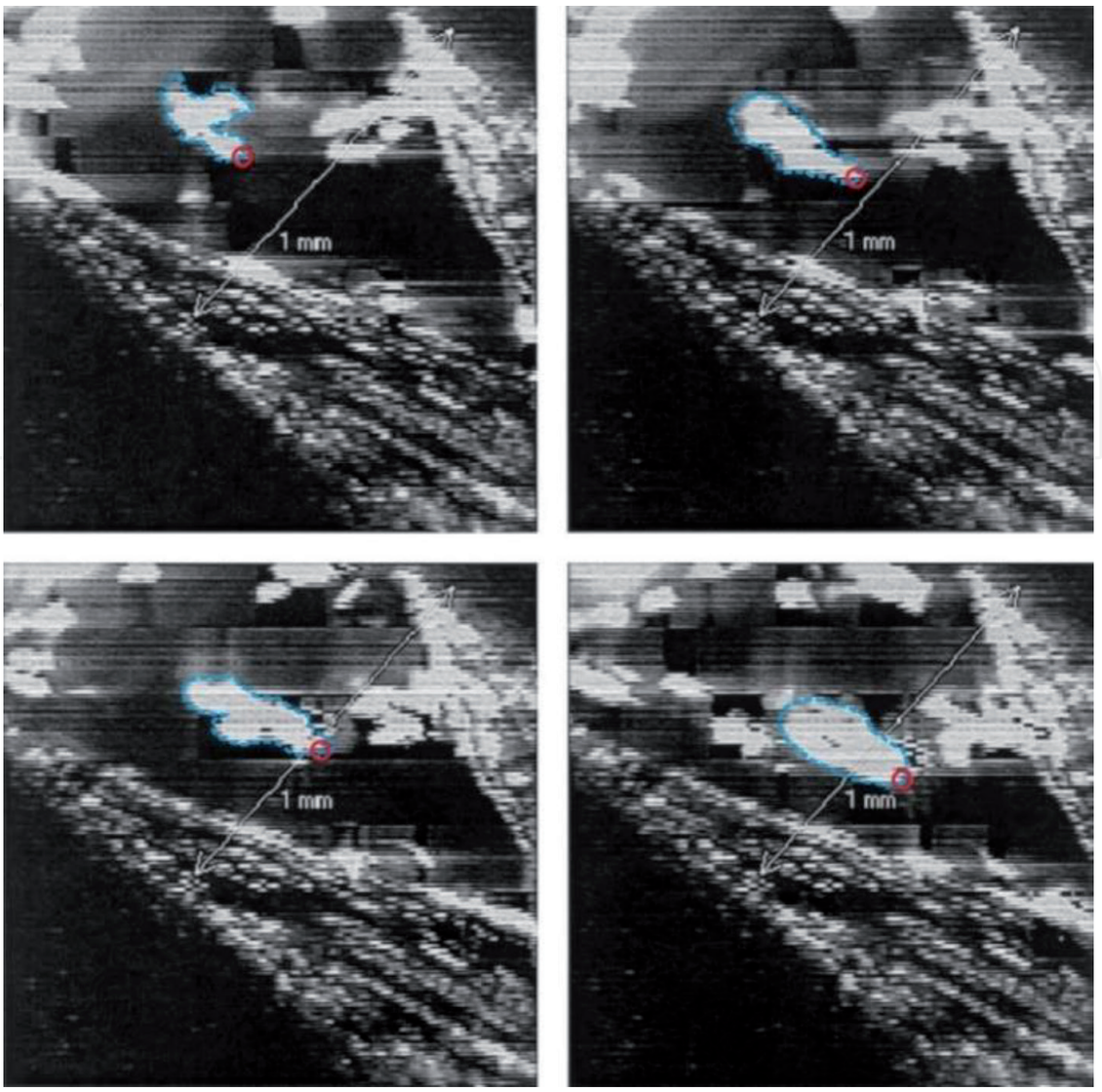

Figure 9.
Four successive images of a hump tip during laser welding [32].

3.4 In suit X-ray imaging

Besides efforts on studying melt surface flow dynamics, internal flows have also been the subject of intensive researches by many researchers. The in situ X-ray transmission imaging technique is a very useful tool to visualize the invisible phenomena in the laser melting sample. The first reported work on X-ray transmission imaging of welding dynamics was in electron beam welding by Arata et al. in 1976 [34]. Later, intensive investigations on keyhole formation [35], keyhole collapse [36], and keyhole porosity formation [37] have been conducted by the laser group in Osaka University around 2000s. **Figure 11** shown the X-ray transmission imaged keyhole melt flow by tracing tungsten particle and porosity formation during laser welding [38]. A more advanced X-ray transmission imaging system based on X-ray tube source was developed by Abt et al. [39] from IFSW, Germany.

Due to the low spectral intensity of X-ray tube, it is hard to observe clear solid–liquid interface. Recently, with the advent of high-flux, high-energy third-generation synchrotrons, X-ray phase contrast imaging is by far the most effective technique for revealing sub-surface structural dynamics with extremely high spatial and temporal resolutions. The knowledge gained are revealing new insights in laser welding and laser additive manufacturing. High-flux, high-energy synchrotron

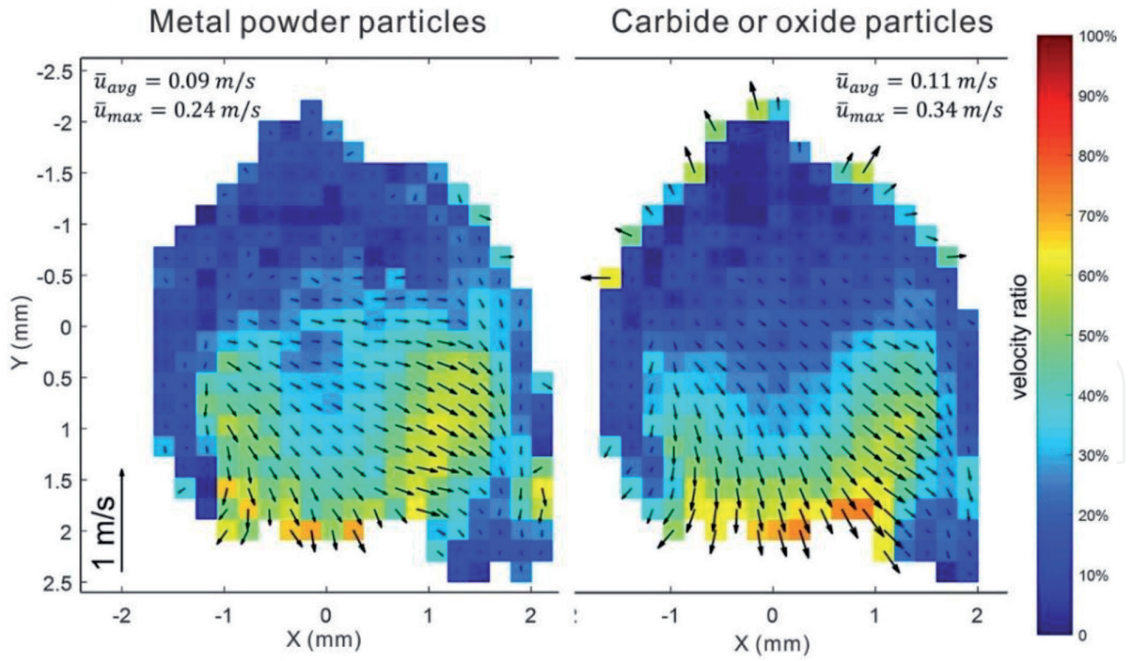

Figure 10.
Resulting metal powder particles (left) and carbide/oxide particles (right) velocity field during L-DED [33].

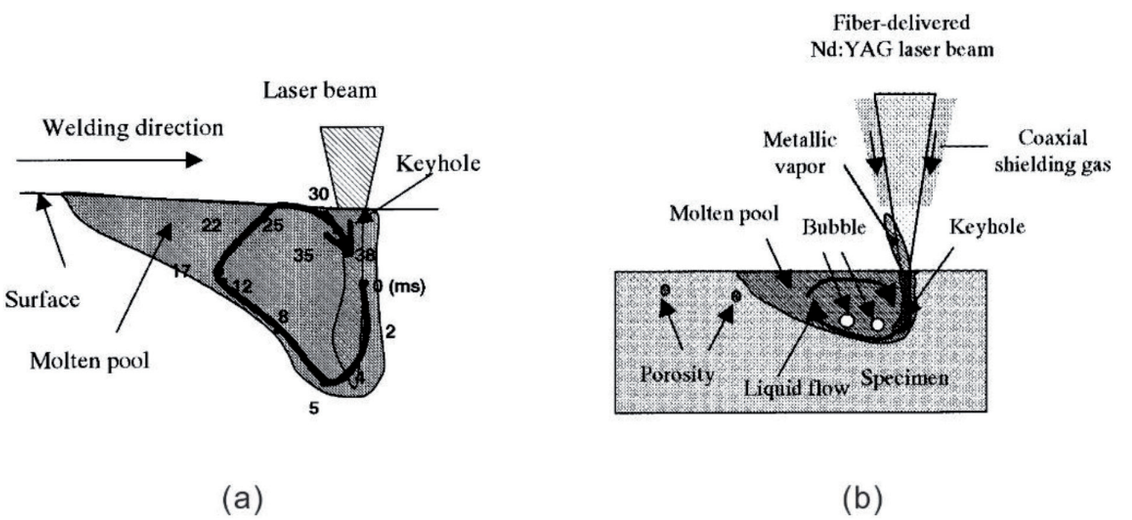

Figure 11.
(a) Keyhole melt flow and (b) porosity formation observed by in situ X-ray transmission imaging setup [38].

X-ray beam source	X-ray energy	Field of view (FOV) (width × height)	Spatial resolution	Time Resolution	References
Super Photon ring-8 GeV (Spring-8), Japan	3–70 keV	24 × 5.1 mm	38 μm	15 ms (70fps)	[40]
Diamond Light Sourcem (DIAMOND), UK	55 keV	8.4× 3.3 mm	6.6 μm	196 μs (5100 fps)	[41]
Stanford Synchrotron Radiation Lightsource (SSRL), USA	24 keV	2.2 × 2.2 mm	1.1 μm	250 us (4000 fps)	[42]
Advanced Photon Source (APS), USA	24.4 keV	1.5 × 1.5 mm	1 μm	100 ps (6500 kfps)	[43]

Table 1.
Several high-speed, high-energy synchrotron facilities used for in situ imaging laser melting process.

X-ray imaging, such as available at the Super Photon ring-8 GeV (Spring-8), Japan, the Diamond Light Source, UK, the Stanford Synchrotron Radiation Lightsource (SSRL), USA and the Advanced Photon Source (APS), USA, has been used to capture the keyhole behavior and defects formation clearly. **Table 1** summaries parameters of these facilities used for in situ imaging laser melting process.

4. Conclusion

In this chapter, we summarized the experimental studies on melt pool flow dynamic during laser material processing, focusing on laser welding and laser additive manufacturing. To visualize the melt pool flow patterns and velocity field, indirect and direct methods have been employed. Indirect methods are simple with low cost, but it can only achieve the final melt flow patterns by postmortem analysis of the cross sections of fusion zones. Direct methods include simulated materials, high speed imaging, and in situ X-ray transmission imaging. These three direct methods need experimental conditions from low cost to expensive, and reveal melt flow information from qualitative to quantify, from surface to internal. This chapter provides a generic guideline for experimental studying melt fluid flow dynamics.

Acknowledgements

The authors acknowledge the support of the National Natural Science Foundation of China (Grant No. 51875190 and 11662010), and Jiangxi National Natural Science Foundation of China (20192BCB23003).

Author details

Xianfeng Xiao[1], Cong Lu[1], Yanshu Fu[1], Xiaojun Ye[1] and Lijun Song[2*]

1 School of Mechatronics Engineering, Nanchang University, Nanchang, Jiangxi, China

2 State Key Laboratory of Advanced Design and Manufacturing for Vehicle Body, Hunan Provincial Key Laboratory of Intelligent Laser Manufacturing, Hunan University, Changsha, China

*Address all correspondence to: ljsong@hnu.edu.cn

References

[1] ASTM F42 Committee: Standard Terminology for Additive Manufacturing Technologies. ASTM International, 2012.

[2] Kou S. Welding Metallurgy. 2nd ed: John Wiley & Sons; 2003.

[3] Staub A, Spierings AB, Wegener K. Correlation of meltpool characteristics and residual stresses at high laser intensity for metal lpbf process. Advances in Materials and Processing Technologies. 2018:1-9.

[4] Yan Z, Liu W, Tang Z, Liu X, Zhang N, Li M, et al. Review on thermal analysis in laser-based additive manufacturing. Optics & Laser Technology. 2018;106:427-41.

[5] Fotovvati B, Wayne SF, Lewis G, Asadi E. A Review on Melt-Pool Characteristics in Laser Welding of Metals. Advances in Materials Science and Engineering. 2018;2018:1-18.

[6] Willy HJ, Li X, Tan YH, Chen Z, Cagirici M, Borayek R, et al. Overview of Finite Elements simulation of temperature profile to estimate properties of materials 3D-printed by Laser Powder-Bed Fusion. Chinese Physics B. 2020;29(4):048101.

[7] K Ishizaki NA, H Murai. Penetration in arc welding and convection in molten metal. Journal of Japan Welding Society. 1965;34:146-53.

[8] Mazumder J. Overview of melt dynamics in laser processing. Optical Engineering. 1991;30(8):1208.

[9] Cook PS, Murphy AB. Simulation of Melt Pool Behaviour during Additive Manufacturing: Underlying Physics and Progress. Additive Manufacturing. 2019;31:100909.

[10] Martin AA, Calta NP, Hammons JA, Khairallah SA, Nielsen MH, Shuttlesworth RM, et al. Ultrafast dynamics of laser-metal interactions in additive manufacturing alloys captured by in situ X-ray imaging. Materials Today Advances. 2019;1:100002.

[11] Srinivasan J, Basu B. A numerical study of thermocapillary flow in a rectangular cavity during laser melting. International Journal of Heat and Mass Transfer. 1986;29(4):563-72.

[12] Chang B, Yuan Z, Pu H, Li H, Cheng H, Du D, et al. A Comparative Study on the Laser Welding of Ti6Al4V Alloy Sheets in Flat and Horizontal Positions. Applied Sciences. 2017;7(4):376.

[13] Guo W, Liu Q, Francis JA, Crowther D, Thompson A, Liu Z, et al. Comparison of laser welds in thick section S700 high-strength steel manufactured in flat (1G) and horizontal (2G) positions. CIRP Annals. 2015;64(1):197-200.

[14] Zhang C, Li X, Gao M. Effects of circular oscillating beam on heat transfer and melt flow of laser melting pool. Journal of Materials Research and Technology. 2020;9(4):9271-82.

[15] CR Heiple HC. Mechanism for Minor Element Effect on GTA Fusion Zone Geometry. Welding Journal. 1982;61(4):97-102.

[16] Sahoo P, Debroy T, McNallan MJ. Surface tension of binary metal—surface active solute systems under conditions relevant to welding metallurgy. Metallurgical Transactions B. 1988;19(3):483-91.

[17] Li D, Lu S, Li D, Li Y. Tracer investigation of convection in weld pool under TIG welding process (in Chinese). Transactions of the China Welding Institution. 2011;32(8):45-8.

[18] Thomy C, Vollertsen F. Influence of Magnetic Fields on Dilution during Laser Welding of Aluminium. Advanced Materials Research. 2005;6-8:179-86.

[19] Zhao L, Sugino T, Arakane G, Tsukamoto S. Influence of welding parameters on distribution of wire feeding elements in CO2laser GMA hybrid welding. Science and Technology of Welding and Joining. 2009;14(5):457-67.

[20] Woods RA, Milner DR. Motion in the weld pool in arc welding. Welding Journal. 1971;50(4):163s-73s.

[21] Andersson D. Streaming due to a thermal surface tension gradient. Scientific Paper No TRITA-EPP-73-19, Royal Institute of Technology, Stockholm, Sweden. 1973.

[22] Ishizaki K. Interfacial tension theory of arc welding phenomena: formation of welding bead. Journal of Japan Welding Society. 1965;34(2):146.

[23] Limmaneevichitr C, Kou S. Visualization of Marangoni convection in simulated weld pools. Welding Journal. 2000;79:126-s.

[24] Limmaneevichitr C, Kou S. Visualization of Marangoni Convection Simulated Weld Pools Containing a Surface-Active Agent. Welding Journal. 2000;79:324-s.

[25] Jin X, Li L. An experimental study on the keyhole shapes in laser deep penetration welding. Optics and Lasers in Engineering. 2004;41(5):779-90.

[26] Kato J, Takamasu K, Ozono S. Investigation of material expulsion mechanism in laser drilling using modelled work piece. Bulletin of the Japan Society of Precision Engineering. 1985;19(2):133-4.

[27] Zhang Y, Li L, Zhang G. Spectroscopic measurements of plasma inside the keyhole in deep penetration laser welding. Journal of Physics D: Applied Physics. 2005;38(5):703.

[28] Semak VV, Hopkins JA, McCay MH, McCay TD. Dynamics of penetration depth during laser welding. Proceedings of ICALEO. 1994:G830-7.

[29] Zhang M, Chen G, Zhou Y, Li S. Direct observation of keyhole characteristics in deep penetration laser welding with a 10 kW fiber laser. Optics express. 2013;21(17):19997.

[30] Huang L, Liu P, Zhu S, Hua X, Dong S. Experimental research on formation mechanism of porosity in magnetic field assisted laser welding of steel. Journal of Manufacturing Processes. 2020;50:596-602.

[31] Ning J, Zhang L-J, Yin X-q, Zhang J-X, Na S-J. Mechanism study on the effects of power modulation on energy coupling efficiency in infrared laser welding of highly-reflective materials. Materials & Design. 2019;178:107871.

[32] Ki H, Mazumder J, Mohanty PS. Modeling of laser keyhole welding: Part II. simulation of keyhole evolution, velocity, temperature profile, and experimental verification. Metallurgical and Materials Transactions A. 2002;33(6):1831-42.

[33] Wirth F, Arpagaus S, Wegener K. Analysis of melt pool dynamics in laser cladding and direct metal deposition by automated high-speed camera image evaluation. Additive Manufacturing. 2018;21:369-82.

[34] Arata Y, Abe E, Fujisawa M. A study on dynamic behaviours of electron beam welding (report I): The observation by a fluoroscopic method. Transactions of Japan Welding Research Institute. 1976:1-9.

[35] Arata Y, Abe N, Oda T. Beam hole behaviour during laser beam welding. Proceedings of ICALEO. 1983;38:59-66.

[36] Matsunawa A, Kim J-D, Seto N, Mizutani M, Katayama S. Dynamics of keyhole and molten pool in laser welding. Journal of Laser Applications. 1998;10(6):247.

[37] Matsunawa A, Kim J, Katayama S. Porosity formation in laser welding mechanisms and suppression methods. Proceedings of ICALEO. 1997:G73-82.

[38] Katayama S, Kobayashi Y, Mizutani M, Matsunawa A. Effect of vacuum on penetration and defects in laser welding. Journal of Laser Applications. 2001;13(5):187.

[39] Abt F, Boley M, Weber R, Graf T, Popko G, Nau S. Novel X-ray System for in-situ Diagnostics of Laser Based Processes – First Experimental Results. Physics Procedia. 2011;12:761-70.

[40] Dorsch F, Terada T, Yamada T, Nishimura A. Development of laser cladding system with process monitoring by x-ray imaging. High-Power Laser Materials Processing: Lasers,Beam Delivery,Diagnostics,and Applications III. 2014;8963:1-10.

[41] Leung CLA, Marussi S, Atwood RC, Towrie M, Withers PJ, Lee PD. In situ X-ray imaging of defect and molten pool dynamics in laser additive manufacturing. Nature Communications. 2018;9(1).

[42] Calta NP, Wang J, Kiss AM, Martin AA, Depond PJ, Guss GM, et al. An instrument for in situ time-resolved X-ray imaging and diffraction of laser powder bed fusion additive manufacturing processes. Review of Scientific Instruments. 2018;89(5):055101.

[43] Parab ND, Zhao C, Cunningham R, Escano LI, Fezzaa K, Everhart W, et al. Ultrafast X-ray imaging of laser–metal additive manufacturing processes. Journal of Synchrotron Radiation. 2018;25(5):1467-77.